When Two-Dimensional Crystals Learn to Remember

This work enables scalable, switchable atomic ferroelectrics, paving the way for ultra-thin, low-power, nonvolatile future electronics.

Two-dimensional (2D) ferroelectrics, which maintain electric polarization at atomic-layer thicknesses, hold significant potential for next-generation electronic devices beyond Moore's law, enabling efficient energy storage and high-density information processing. In naturally occurring van der Waals crystals such as hexagonal boron nitride (h-BN) and transition-metal dichalcogenides, ferroelectricity is absent because these materials favor centrosymmetric stacking configurations with lower formation energy. This limitation was addressed by mechanically exfoliating and restacking h-BN layers with controlled rotational and translational offsets, thereby breaking inversion symmetry and inducing out-of-plane polarization. The discovery of ferroelectricity in twisted h-BN has sparked broad interest in symmetry-breaking phenomena, including giant piezoelectricity and ferroelectricity in other layered materials. For practical device applications, scalable and controllable synthesis of ferroelectric h-BN is crucial.

Chemical vapor deposition (CVD) is a promising bottom-up method for producing large-area, high-quality h-BN films and is widely used for 2D dielectrics. However, epitaxial growth of multilayer h-BN with polarized stacking on inert or non-metal substrates remains highly challenging, as CVD growth typically favors non-polar configurations and lacks catalytic support after monolayer formation.

Unlike CVD, which relies on substrate catalysis, molecular beam epitaxy (MBE) is well suited for the controlled growth of multilayer structures due to its precise flux control and *in situ* reflection high-energy electron diffraction (RHEED) monitoring. In this work, Chung-Lin Wu (National Cheng Kung University), Cheng-Maw Cheng (NSRRC), and their teams used the nitrogen plasma-assisted MBE (PA-MBE) method to directly grow layer-controlled hexagonal boron nitride (h-BN) on lattice-matched graphene formed on

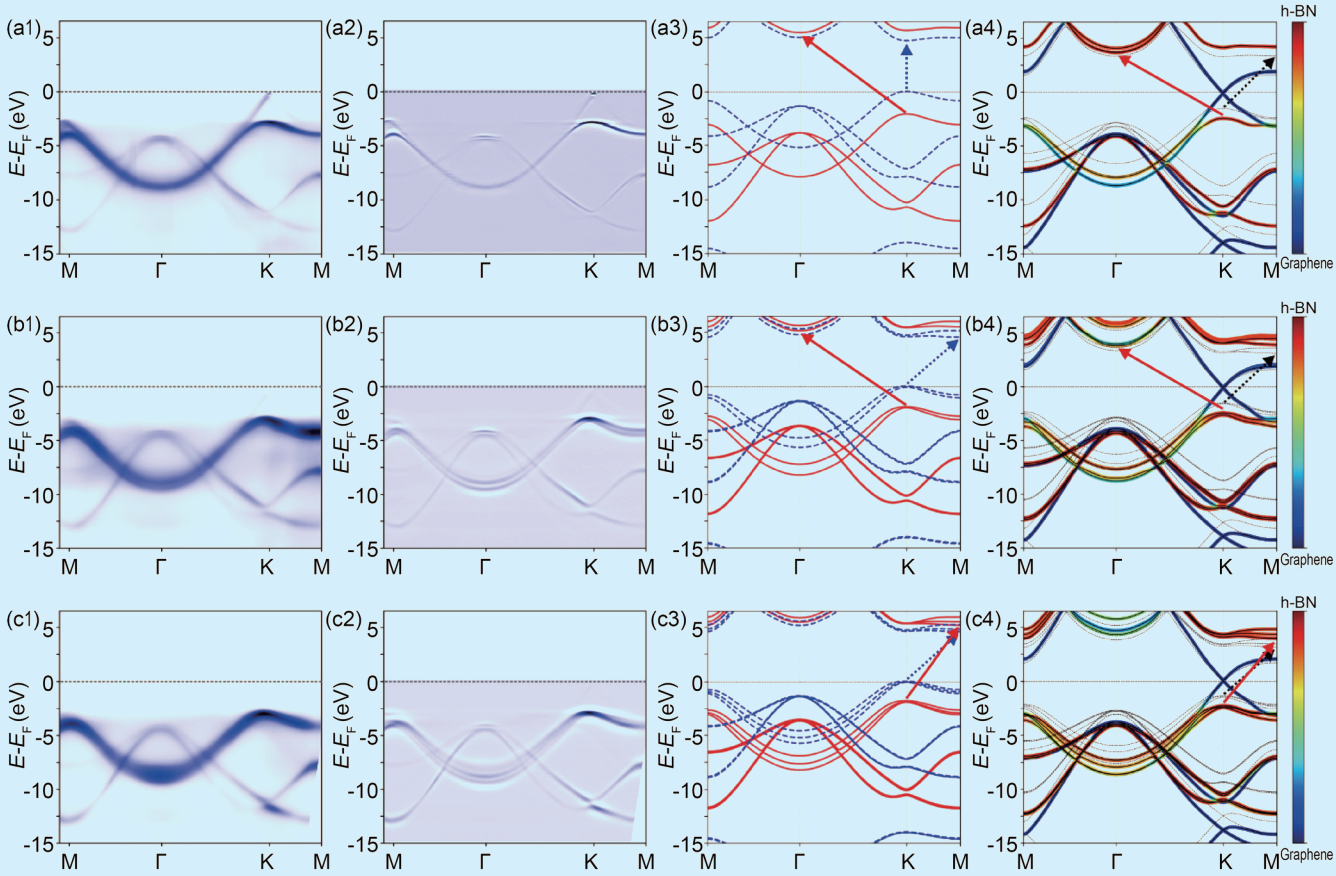

Fig. 1: Electronic band structures of h-BN and h-BN/graphene. (a1–c1) ARPES spectra of mono-, bi- and tri-layer h-BN/graphene. (a2–c2) The corresponding 2nd derivatives of ARPES data in (a1–c1). (a3–c3) Electronic band structures of free-standing mono-, bi-, and tri-layer h-BN calculated at the density function theory (blue dashed curves) and GW (red solid curves) levels. (a4–c4) Orbital-projected GW band structures for h-BN (red) and graphene (blue) lateral heterostructures. [Reproduced from Ref. 1]

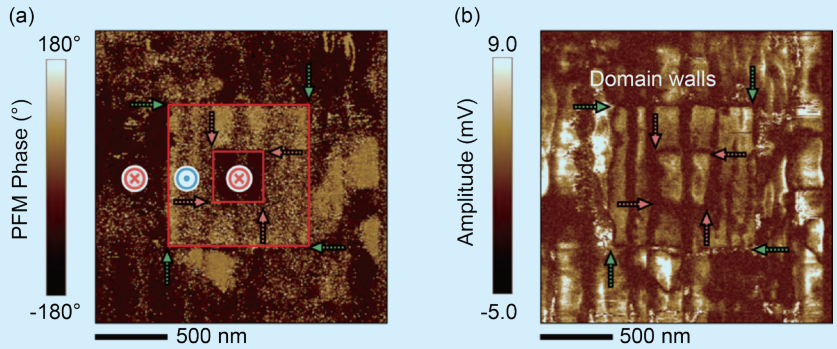

Fig. 2: Box-in-box pattern (+5 V/1000×1000 nm², −6 V/400×400 nm²) on 3 MLs h-BN sample. (a) Phase and (b) amplitude images of the box-in-box pattern on a 3 ML h-BN sample. [Reproduced from Ref. 1]

a commercially available 4H-SiC (0001) substrate with a 4° miscut. After ultra-high-vacuum annealing, high-quality multilayer graphene with step edges along the $\langle 1\bar{1}20 \rangle$ direction was epitaxially grown, as confirmed by streak RHEED patterns. Under nitrogen-rich conditions, N_2 plasma enhances boron surface diffusion, enabling h-BN growth at temperatures significantly lower than those required for CVD. Scanning probe and electron microscopy reveal smooth, continuous monolayer h-BN covering atomically flat graphene terraces and extending across step edges. Preferential nucleation at step edges promotes aligned bilayer island growth and seamless island merging, resulting in high-quality layer-by-layer h-BN films. Raman spectroscopy further confirms the exceptional crystalline quality of the grown h-BN.

To deepen the understanding of the stacked sequence, they performed angle-resolved photoemission spectroscopy (ARPES) at the **TLS 21B1** high-resolution photoemission spectroscopy beamline. The high crystalline quality and uniform stacking order of the layer-controlled h-BN films are confirmed by the excellent agreement between ARPES measurements and layer- and stacking-dependent GW band-structure calculations. The chemically inert nature of MBE-grown h-BN enables reliable *ex situ* ARPES measurements without protective capping layers. ARPES spectra of mono-, bi-, and trilayer h-BN along high-symmetry directions in the Brillouin zone reveal clear layer-dependent band dispersions. Although graphene π bands from the underlying substrate contribute to the spectra, characteristic features such as band splitting near the K point confirm the Bernal stacking of multilayer graphene. Distinct parabolic dispersions appear in bi- and trilayer h-BN due to interlayer coupling, providing a direct spectroscopic fingerprint of layer number and validating the layer-by-layer growth mode achieved by PA-MBE. Comparison with GW calculations further shows that the experimental spectra of bilayer and trilayer h-BN are consistent with polarized AB and ABA stacking configurations, respectively, while non-polarized stacking orders are excluded based on clear discrepancies in band dispersions. The spatial uniformity of band structures across different beam positions, together with second harmonic generation measurements, demonstrates homogeneous, millimeter-scale epitaxial growth with a polarized stacking configuration.

To elucidate the epitaxial growth mechanism, density functional theory calculations were performed to evaluate the formation energies of h-BN on graphene with various surface morphologies. Supported by high-resolution scanning transmission electron microscope imaging, the calculations show that graphene step edges, particularly concave regions, significantly lower the interfacial formation energy and serve as thermodynamically favorable nucleation sites. This step-guided conformal epitaxy accounts for the mono-oriented, polarized stacking of h-BN observed experimentally.

Furthermore, ferroelectricity in multilayer h-BN films was investigated using piezoresponse force microscopy (PFM) on Bernal-stacked graphene substrates. An OFF-field measurement protocol was employed to eliminate electrostatic artifacts and probe intrinsic polarization. Clear 180° phase reversals between bilayer and trilayer regions reveal layer-dependent polarization stacking driven by moiré and Bernal configurations. Applying a biased probe induces interlayer sliding, enabling reversible polarization switching characteristic of sliding ferroelectricity. Both bilayer and trilayer h-BN exhibit butterfly-shaped PFM amplitude loops and sharp phase switching at coercive voltages of ~±1.5 V, with trilayers showing the largest saturated response. Kelvin probe force microscopy confirms a stable ~300 meV surface potential contrast after switching, persisting for at least one week. Domain writing experiments demonstrate robust, damage-free polarization control, with trilayer h-BN offering superior uniformity and stability. These results establish epitaxial multilayer h-BN as a scalable, durable 2D ferroelectric platform. This work addresses key challenges in 2D ferroelectricity—scalability, stability, and switchability—by developing bottom-up, layer-by-layer epitaxial growth of hexagonal boron nitride (h-BN). A step-edge-guided process enables large-area, polar-stacked multilayer h-BN on h-BN/graphene moiré structures. As in graphene epitaxy, symmetry breaking at substrate steps is crucial for forming non-centrosymmetric van der Waals crystals. The resulting sliding ferroelectricity in h-BN, combined with the electronic, magnetic, and photonic properties of vdW materials, creates new opportunities for nonvolatile, reconfigurable 2D devices and multifunctional heterostructures. (Reported by Cheng-Maw Cheng)

*This report features the work of Chung-Ling Wu, Cheng-Maw Cheng and their collaborators published in Adv. Mater. **37**, 2414442 (2025).*

TLS 21B1 Angle-resolved UPS

- Angle-resolved Photoemission Spectroscopy
- Materials Science, Condensed-matter Physics

Reference

1. S.-S. Wong, Z.-Y. Lin, S.-Z. Ho, C.-E. Hsu, P.-H. Li, C.-Y. Chen, Y.-F. Huang, K.-E. Chang, Y.-C. Hsieh, C.-H. Chen, M.-H. Lee, M.-W. Chu, K.-I Lin, T.-M. Chen, Y.-C. Chen, H.-C. Hsueh, C.-M. Cheng, C.-L. Wu, Adv. Mater. **37**, 2414442 (2025).

Peeling Ferroelectrics to Power the Next Electronics Revolution

Freestanding ferroelectric membranes unlock CMOS-ready, low-power two-dimensional transistors and enable scalable logic for next-generation three-dimensional electronics.

As silicon-based complementary metal–oxide–semiconductor (CMOS) technology approaches its physical scaling limits, further transistor miniaturization faces increasing challenges such as heat dissipation and carrier mobility degradation. Two-dimensional (2D) semiconductors, with their atomically thin bodies and excellent electrostatic control, offer a promising alternative channel material for next-generation electronics. A critical bottleneck, however, is the integration of high-quality, high-κ gate dielectrics into 2D materials. Conventional atomic layer deposition often produces amorphous oxides and defective interfaces on 2D surfaces, while buffer-layer approaches can degrade dielectric performance. Although van der Waals insulators such as hexagonal boron nitride improve interfaces, their integration with CMOS processes remains difficult.

To overcome the barrier of integration with CMOS-compatible high-κ dielectrics, Jan-Chi Yang (National Cheng Kung University), Yen-Fu Lin (National Chung Hsing University), and their teams establish a reliable route to fabricate high-quality freestanding ferroelectric $Hf_{0.5}Zr_{0.5}O_2$ (HZO) membranes and systematically investigate their structural and electronic properties prior to integration with two-dimensional semiconductors. The freestanding HZO membranes are produced by selectively etching a sacrificial $La_{0.7}Sr_{0.3}MnO_3$ (LSMO) layer from epitaxial LSMO/HZO heterostructures grown on single-crystal $SrTiO_3$ substrates. They fabricated freestanding ferroelectric HfO_2-based oxides doped with zirconium (HZO) membranes using pulsed laser deposition and integrated with few-layer MoS_2 field-effect transistors (FETs). The membranes are produced by epitaxially growing an LSMO/HZO heterostructure on $SrTiO_3$, followed by selective chemical removal of the sacrificial LSMO layer. This approach yields mechanically intact membranes suitable for transfer without compromising crystallinity or ferroelectric functionality. Electrical characterization reveals that 20-nm-thick freestanding HZO membranes possess a high dielectric constant (~20.6), a large breakdown field (~2.2 MV cm^{-1}), and robust ferroelectric polarization.

High-resolution transmission electron microscopy reveals well-ordered atomic lattices in 20-nm-thick freestanding HZO membranes, dominated by the orthorhombic (o-) phase, which is responsible for ferroelectricity. Atomic force microscopy

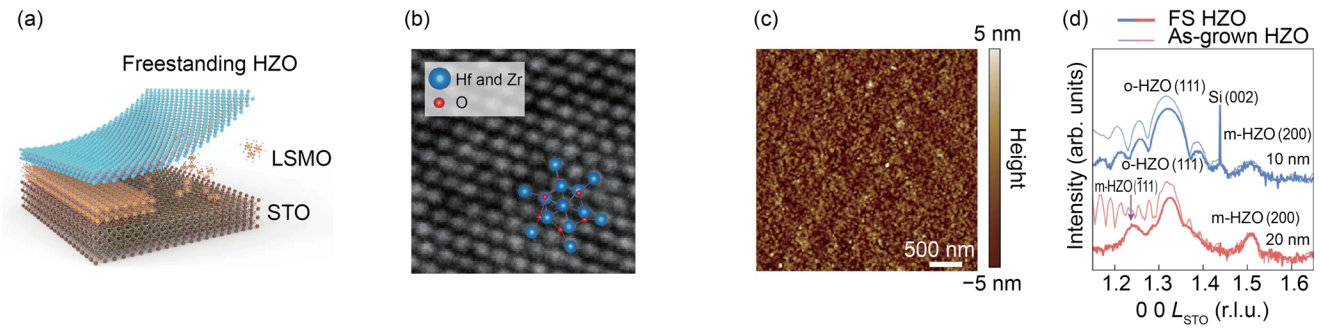

Fig. 1: Fabrication and characterization of ferroelectric freestanding HZO membranes. (a) Schematic of the fabrication process for freestanding HZO membranes. (b) Transmission electron microscopy image showing the o-phase (111) of freestanding HZO with the corresponding lattice model. (c) AFM image of a 20-nm freestanding HZO membrane, with an Ra value of 0.86 nm. (d) Comparison of XRD θ–2θ scans between as-grown and freestanding HZO membranes at thicknesses of 10 and 20 nm. [Reproduced from Ref. 1]